MOLECULAR AND CELLULAR BIOLOGY, July 1996, p. 3934–3944 Vol. 16, No. 7
0270-7306/96/$04.00+0

Alpha Interferon Suppresses the Cyclin D3 and *cdc25A* Genes, Leading to a Reversible G_0-Like Arrest

NAVA TIEFENBRUN,[1] DROR MELAMED,[1] NAOMI LEVY,[1] DALIA RESNITZKY,[2,3] INGRID HOFFMANN,[4] STEVEN I. REED,[3] AND ADI KIMCHI[1]*

Departments of Molecular Genetics[1] and Molecular Cell Biology,[2] The Weizmann Institute of Science, Rehovot 76100, Israel; Department of Molecular Biology, Scripps Research Institute, La Jolla, California 92037[3]; and Department of Applied Tumor Virology, German Cancer Research Center, 69120 Heidelberg, Federal Republic of Germany[4]

Received 11 January 1996/Returned for modification 20 March 1996/Accepted 19 April 1996

Alpha interferon is a potent growth inhibitor of Daudi Burkitt's lymphoma cells. We show here that alpha-interferon signaling interacted simultaneously with several components of the basic cell cycle machinery, causing cells to enter into a state that had many features characteristic of the G_0 state. Within a few hours after alpha-interferon treatment, cyclin D3 mRNA and protein levels dropped to undetectable levels and, in parallel, the activities of cyclin A- and cyclin E-associated kinases were significantly reduced. The latter resulted from the rapid alpha-interferon-mediated elimination of cdc25A, a phosphatase that is required for antagonism of negative tyrosine phosphorylation of cdk2 in cyclin-cdk complexes. This regulation represents a novel mechanism through which an external inhibitory cytokine interacts with the cell cycle machinery. At later time points after alpha-interferon treatment, the levels of the 55-kDa slowly migrating hyperphosphorylated form of cyclin E and of cyclin A were also reduced. The antiproliferative effects were reversible, and cultures from which alpha interferon was removed reentered S phase after a lag that typically corresponded to approximately two doubling times. During this lag period, the expression of cyclin D3 and cyclin A, as well as of the cdc25A phosphatase, continued to be switched off, in spite of the removal of alpha interferon from the cell surface. In contrast, c-*myc*, which represents another downstream target gene that is subjected to negative regulation by alpha interferon, was relieved from suppression much earlier, concomitant with the decay in early signaling of the cytokine. The delayed pattern of cyclin reexpression provides evidence that alpha-interferon signaling imposes a G_0-like state on this system.

The arrest of cell proliferation is an active process that can be induced by growth-inhibitory cytokines, of which alpha interferon (IFN-α) is an example (for a review, see reference 18). Exponentially growing cultures of Daudi Burkitt's lymphoma or M1 myeloid cells that have been exposed to IFN-α accumulate mostly in a state in which they carry a 2*n* DNA content, previously referred to, without further characterization, as the G_0/G_1 phase (6, 19). A few specific interactions between the receptor-generated signaling cascades of IFN-α and cell-cycle-controlling genes have been identified in the past. The c-*myc* gene was identified as one of the first downstream targets on the basis of the observation that c-*myc* mRNA expression in these hematopoietic cells was suppressed by IFN-α (6, 19). Transcriptional suppression of c-*myc* in these cells was attributed at least partially to an IFN-α-dependent reduction in the DNA-binding activity of the transcription factor E2F to its cognate site in the c-*myc* promoter (25). Disruption of c-*myc* suppression by the ectopic expression of deregulated c-*myc* interfered with the ability of IFN-α to arrest the cells specifically in the G_0/G_1 phase. Yet, this genetic manipulation did not restore the full proliferative activity of the cells, which suggested that additional molecular pathways continued to be rate limiting in the system (33). The pRB protein was then identified as a second independent target of IFN-α signaling. Activation of pRB by IFN-α through the suppression of its phosphorylation complemented the partial cell cycle arrest mediated by c-*myc* inhibition (34). Since pRB is phosphorylated by the cyclin-dependent kinases (14, 31), we hypothesized that the pRB responses might be the result of negative regulation of the major cell cycle kinases that control entry into S phase by IFN-α signaling, an issue addressed in this work.

While investigating the molecular mechanisms that mediate inhibition of cell proliferation by IFNs, it was important, in addition, to determine the precise nature and characteristics of the growth-arrested cell population. For example, it was not known whether IFN-α-treated cells accumulate at a late checkpoint in G_1 similar to that described for transforming growth factor β (TGF-β)-induced cell cycle arrest (16) or, alternatively, whether they leave the cell cycle and enter into a G_0-like resting state. Experiments that follow the reentry of cells into the cell cycle after removal of the proliferation constraints induced by the cytokine were therefore undertaken to address this issue.

We show here that the cyclin D3 and *cdc25A* genes are primary targets of IFN-α signaling and that the suppression of cdc25A phosphatase is the cause of the inhibitory effects of IFN-α on the activities of cyclin E- and cyclin A-associated kinases. The cytokine-treated cultures became reversibly blocked in a G_0-like state. Interestingly, preceding S-phase reentry, there was a prolonged lag during which the expression of the cyclin and *cdc25A* genes continued to be switched off in spite of the removal of IFN-α from the cell surface. In contrast, c-*myc* reexpression occurred much more rapidly, concomitant with the decline in the early signaling of IFN-α. This delay in cyclin and *cdc25A* gene expression provides an important fea-

* Corresponding author. Mailing address: Department of Molecular Genetics, The Weizmann Institute of Science, Rehovot 76100, Israel. Phone: 972-8-9342428. Fax: 972-8-9344108.

ture that characterizes the G_0-like state that is induced by IFN-α in Daudi cells.

MATERIALS AND METHODS

Cells, culture conditions, and cytokine treatment. Daudi Burkitt's lymphoma cells were grown in RPMI 1640 medium (Bio-Lab, St. Paul, Minn.) supplemented with 10% (vol/vol) heat-inactivated (56°C) fetal calf serum (Bio-Lab). Under these conditions, the cell doubling time was 24 h. Cell viability was determined by trypan blue exclusion tests. Human IFN-α was purified to 5×10^8 U/mg by affinity chromatography with monoclonal antibodies as described previously (6). Cells were routinely treated with 300 U of IFN-α per ml for 48 h.

Flow cytometric analysis. Cell cycle analysis was performed with a FACScan (Becton-Dickinson). The procedures for DNA staining with propidium iodide (PI), labeling of S-phase cells with antibromodeoxyuridine (anti-BrdU) antibodies, and determination of protein content with fluorescein isothiocyanate (FITC) were detailed previously (23).

Northern (RNA) blot analysis and probes. Total cellular RNA was extracted by using Tri-Reagent (Molecular Research Center, Inc.). Poly(A)$^+$ RNA was purified by using Dynabeads Oligo $(dT)_{25}$ (Dynal, Inc.). RNA was electrophoresed on formamide-formaldehyde agarose gels, transferred onto Hybond-N membranes (Amersham), and processed as previously described (40). Hybridization was performed with 10^6 cpm of each of the following ^{32}P-labeled DNA probes per ml: a 1.6-kb *Eco*RI fragment of the murine *cyl3* cDNA (24), a 2.5-kb *Spe*I-*Xba*I fragment of cyclin E cDNA, a 1-kb *Bam*HI-*Nde*I fragment of human cyclin A cDNA, a 2.3-kb *Eco*RI fragment of human *cdc25A* cDNA, and a 1.3-kb *Pst*I fragment of rat glyceraldehyde-3-phosphate dehydrogenase cDNA.

Immunoblot analysis and immunoprecipitations. For detection of proteins on immunoblots, whole-cell extracts were prepared as described previously (23). Samples containing 100 μg of protein were fractionated on sodium dodecyl sulfate (SDS)–7.5% polyacrylamide gels and electroblotted onto a nitrocellulose filter in blotting buffer (33 mM Tris, 192 mM glycine, 20% [vol/vol] methanol). For the detection of cyclin D3 and cdk2, 12% acrylamide gels were used. The filter was blocked for 2 h in blocking solution (10% lowfat milk in phosphate-buffered saline [PBS] containing 0.5% Tween 20) and then was incubated for an additional 2 h with the specific antibodies. Following extensive washing with PBS containing 0.5% Tween 20, the filter was incubated for 45 min with peroxidase-conjugated protein A or peroxidase-conjugated goat anti-mouse antibodies. The filter was extensively washed, and bound antibodies were visualized by using the enhanced chemiluminescence Western blotting system (Amersham).

For immunoprecipitation, cells were lysed in modified radioimmunoprecipitation assay buffer (mRIPA) (0.5% sodium deoxycholate, 0.5% Triton X-100, 150 mM NaCl, 50 mM Tris [pH 7], 5 mM EDTA) containing 20 mM NaF, 100 mM $NaVO_4$, and protease inhibitors (1 mM phenylmethylsulfonyl fluoride, 50 μg of aprotinin per ml, 50 μg of leupeptin per ml, 7.5 μg of pepstatin A per ml, 10 μg of antipain per ml, and 10 μg of chymostatin per ml). Protein concentration was determined by using the Bio-Rad protein assay. Immunoprecipitations of protein lysates were performed with polyclonal antibodies directed against cyclin A (1 μl per 100 μg of extract), polyclonal antibodies directed against cdk2 (5 μl per 100 μg of extract), and monoclonal antibodies directed against cyclin E (100 μl per 800 μg of extract). Immune complexes were adsorbed onto protein A-Sepharose beads and were extensively washed.

To assay cdk2-cyclin A association, anti-cyclin A immune complexes were recovered from 400 μg of protein lysate, washed three times with mRIPA, and incubated with 2× sample buffer (4% SDS, 20% glycerol, 120 mM Tris [pH 6.8], 10% β-mercaptoethanol, and bromophenol blue) at 37°C for 10 min. Samples were resolved by SDS-polyacrylamide gel electrophoresis (SDS-PAGE; 11% gel) and immunoblotted. The upper part of the gel was probed with anti-cyclin A antibodies, and the lower part was probed with anti-cdk2 antibodies.

Cyclin-associated H1 kinase activity assay. Prior to performance of the kinase assay, immune complexes were washed with mRIPA, 0.5 M LiCl, and reaction buffer (20 mM Tris [pH 7.5], 7.5 mM $MgCl_2$). The beads were then resuspended in 5 μl of a kinase assay mixture consisting of reaction buffer, 80 μM [γ-^{32}P]ATP, histone H1 (7.5 μg) (Boehringer Mannheim), and protease inhibitor cocktail. After incubation of the beads at 37°C for 30 min, the reaction was stopped by the addition of 2× Laemmli gel sample buffer. Proteins were separated by electrophoresis on an 11% polyacrylamide gel. Histone H1 was visualized by Coomassie blue staining, and the gel was destained by incubation in 10% acetic acid and then dried. The histone-incorporated radioactivity was quantitated with a phosphoimager (Fujix BAS-1000; Fuji).

cdc25 phosphatase assay. Glutathione *S*-transferase (GST)–cdc25 fusion protein was expressed and purified essentially as described previously (27). Protein recovery was determined by Coomassie blue staining of SDS–7.5% polyacrylamide gels with bovine serum albumin (BSA) as the standard. Phosphatase activity was calibrated with *p*-nitrophenyl-phosphate as a substrate according to the procedure of Millar et al. (27). The in vitro assay with GST-cdc25 was performed after immunoprecipitation of protein lysates with anti-cyclin A, anti-cyclin E, and anti-cdk2 as described above. Immune complexes were washed with mRIPA, 0.5 M LiCl, and phosphate buffer (PB) containing 5 mM EDTA, 2 mM spermidine, 2 mM dithiothreitol, and 25 mM MOPS (morpholinepropanesulfonic acid) (pH 7.2). The supernatant was aspirated, and the beads were incubated with 50 μl of PB containing 0.1% BSA and 100 μg of GST-cdc25 or GST alone per ml at 30°C for 30 min. The reaction was stopped by washing the beads several times in reaction buffer (20 mM Tris-HCl [pH 7.5], 7.5 mM $MgCl_2$), and the histone H1 kinase assay was performed as described above.

Antibodies. The antibodies used for immunoblotting analysis and immunoprecipitation were as follows: monoclonal antibodies against a myc synthetic peptide that corresponds to amino acids 173 to 188 of human c-myc, collected from the supernatant of hybridoma MYC1-3C7 (8); a polyclonal antiserum generated against a bacterially produced human cyclin A (32); affinity-purified anti-cyclin A polyclonal antibodies (28); monoclonal antibodies against recombinant human cyclin D3 (clone G107-565; PharMingen); monoclonal antibodies against human cyclin E (clone HE12 for Western blot [immunoblot] analysis and HE111 for immunoprecipitation) (22); polyclonal antibodies against human cdk2 (a gift from G. Draetta); anti-IRF-1 polyclonal antibodies (a gift from J. Chebath and S. Harroch); monoclonal antibodies against vinculin (Sigma Immunochemicals); and affinity-purified rabbit polyclonal antibodies generated against a peptide corresponding to the N-terminal region of the cdc25A protein (15).

RESULTS

Initial characterization of the type of proliferation arrest that is induced by IFN-α in Daudi cells. Exponentially growing cultures of human Daudi Burkitt's lymphoma cells were exposed to IFN-α (300 U/ml), after which the cell cycle distribution was analyzed. This was performed by the double staining of BrdU-pulse-labeled cells with PI and fluorescent anti-BrdU antibodies, a method which provides a clear distinction between cells that are engaged in active DNA synthesis (e.g., in Fig. 1A, part a, 53% of the exponentially growing cell culture) and those that do not incorporate the BrdU precursor and have DNA contents that are consistent with the G_1 (2*n*) or G_2/M (4*n*) phase. No change in cell cycle distribution was apparent during the first 8 h following exposure to IFN-α. An increase in the fraction of 2*n*-DNA-containing cells was noticeable between 8 and 16 h, and this fraction continued to expand with additional incubation (Fig. 1B). By 48 h, 85% of the cells were arrested with 2*n* DNA contents while the rest of the population still continued to traverse the S (BrdU positive) and G_2/M phases (Fig. 1A, part b). The residual fraction of cycling cells (S + G_2 + M = 15%) eventually joined the pool of 2*n*-DNA-containing cells during the next 24 h (Fig. 1B).

The protein contents of cells were then measured as an indirect parameter for testing whether the 2*n*-DNA-containing cells were blocked by IFN-α in late G_1. The protein contents of cells were determined as a function of their cell cycle distributions by double staining of DNA and protein with PI and FITC, respectively. In logarithmic-phase cultures, about 65% of G_1 cells had protein contents that were equivalent to those found in the S and G_2 replicating phases while the remaining 35%, representing early stages of the G_1 phase, contained lower protein levels (the population below the solid line in Fig. 1C, part a). Interestingly, the 2*n*-DNA-containing cells from the IFN-α-treated cell population displayed on average a marked drop in FITC staining (about 60% of 2*n*-DNA-containing cells were below the solid line in Fig. 1C, part b), some of them reaching levels that were far below the minimum values measured in the early-G_1 cells from cycling cultures (the population below the dashed line in Fig. 1C, part b). A second feature that changed in these nonproliferating cells was cell size, as determined by the forward scatter of the fluorescence-activated cell sorter (FACS) laser beam. As shown in Fig. 1D, the average cell size was greatly reduced after IFN-α treatment. The reduced values for protein content and cell size excluded the possibility that the IFN-α-induced cell cycle arrest occurred in late G_1 phase.

IFN-α inhibits the expression of cyclin D3 and reduces the slowly migrating form of the cyclin E protein. We studied whether the expression of either cyclin D or cyclin E was affected by IFN-α signaling, leading to the arrest of proliferation. Of the different members of the cyclin D family, only

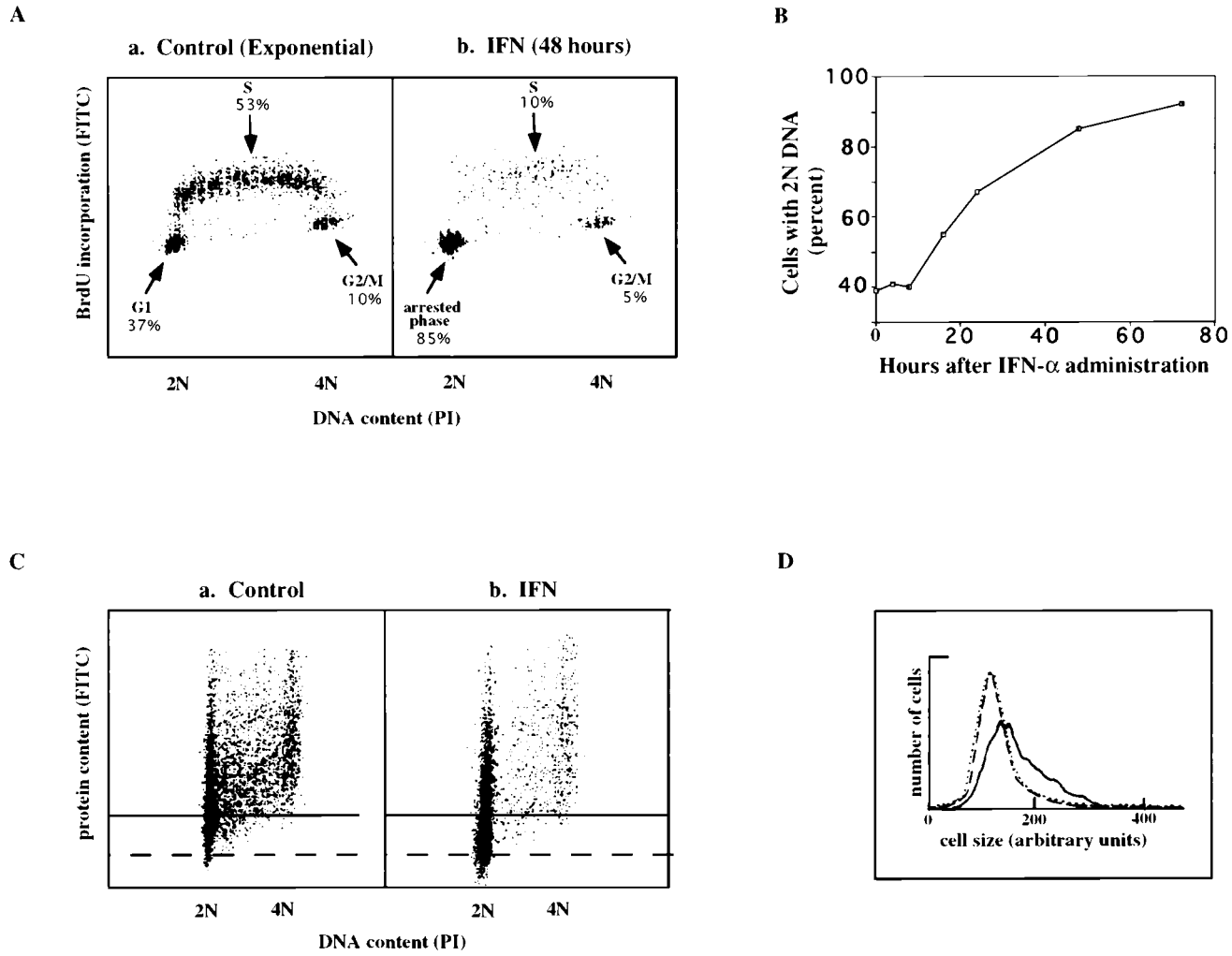

FIG. 1. Cytofluorimetric characterization of IFN-α-treated Daudi cells. (A) Cycling cells in logarithmic phase (part a) and cells treated with IFN-α (300 U/ml) for 48 h (part b) were pulsed-labeled with BrdU, fixed, double stained with FITC-conjugated anti-BrdU antibodies and PI, and subjected to FACS analysis. The percentages of cells in the different cell cycle phases are indicated. Note the accumulation of 2*n*-DNA-containing cells in the treated culture (arrested phase). (B) The cells were double stained with anti-BrdU antibodies and PI at different time intervals after IFN-α treatment, and the percentage of nonreplicating 2*n*-DNA-containing cells was calculated. (C) Control cells (part a) and cells that were treated with IFN-α for 48 h (part b) were double stained with FITC and PI for the determination of protein and DNA content, respectively. The minimum protein content threshold of the cycling phases (the lower FITC signal in 4*n*-DNA-containing cells) is depicted by a solid line. An arbitrary reference was set (dashed line) for the visualization of the decline in protein content and of the appearance of a new cell population in the IFN-α-treated cells. (D) The distribution of forward-scatter intensities as a measure of cell size. The forward-scatter intensities of samples from control cells (solid line) and cells continuously treated with IFN-α for 48 h (dotted-dashed line) were analyzed.

cyclin D3 is expressed by exponentially growing Daudi cells. In response to IFN-α, cyclin D3 mRNA levels were rapidly reduced (Fig. 2A). The steady-state levels of the protein were measured on immunoblots, and as expected from the RNA data and consistent with the short half-life of the protein, cyclin D3 protein levels dropped very rapidly after the exposure of Daudi cells to the cytokine (Fig. 2B). Considerable levels of reduction were apparent at the 4-h point, and maximal suppression was observed a few hours later. The kinetics of cyclin D3 protein reduction were similar to the previously described kinetics of c-myc protein suppression in this system (34).

Cyclin E mRNA levels were also reduced by IFN-α but with slower kinetics than were observed for the cyclin D3 mRNA (Fig. 2A). However, a more rapid response to IFN-α was observed at the protein level. Two major forms of cyclin E were detected on immunoblots, and they were 50 and 55 kDa in size. Previous work, performed in other cell systems, suggested that the 55-kDa protein represents the hyperphosphorylated cyclin E, on the basis of in vitro phosphatase assays. The finding that this slowly migrating form was present exclusively in active kinase complexes suggested that it either was involved in kinase activation or was a marker for activated kinase (4). More recent data support the latter hypothesis (39). The immunoblot in Fig. 2B shows that the two forms of cyclin E had different responses to IFN-α. The levels of the 55-kDa species were reduced by 8 h after IFN-α treatment (i.e., the reduction in protein preceded the mRNA response) and remained low thereafter. In contrast, the steady-state levels of the 50-kDa underphosphorylated form of cyclin E did not change during the entire course of IFN-α treatment, even at the time points at which the mRNA was strongly suppressed, suggesting that this form has a long half-life. Finally, consistent with our previous data (34), cyclin A protein levels were also reduced in Daudi cells but with slower kinetics which paralleled the timing

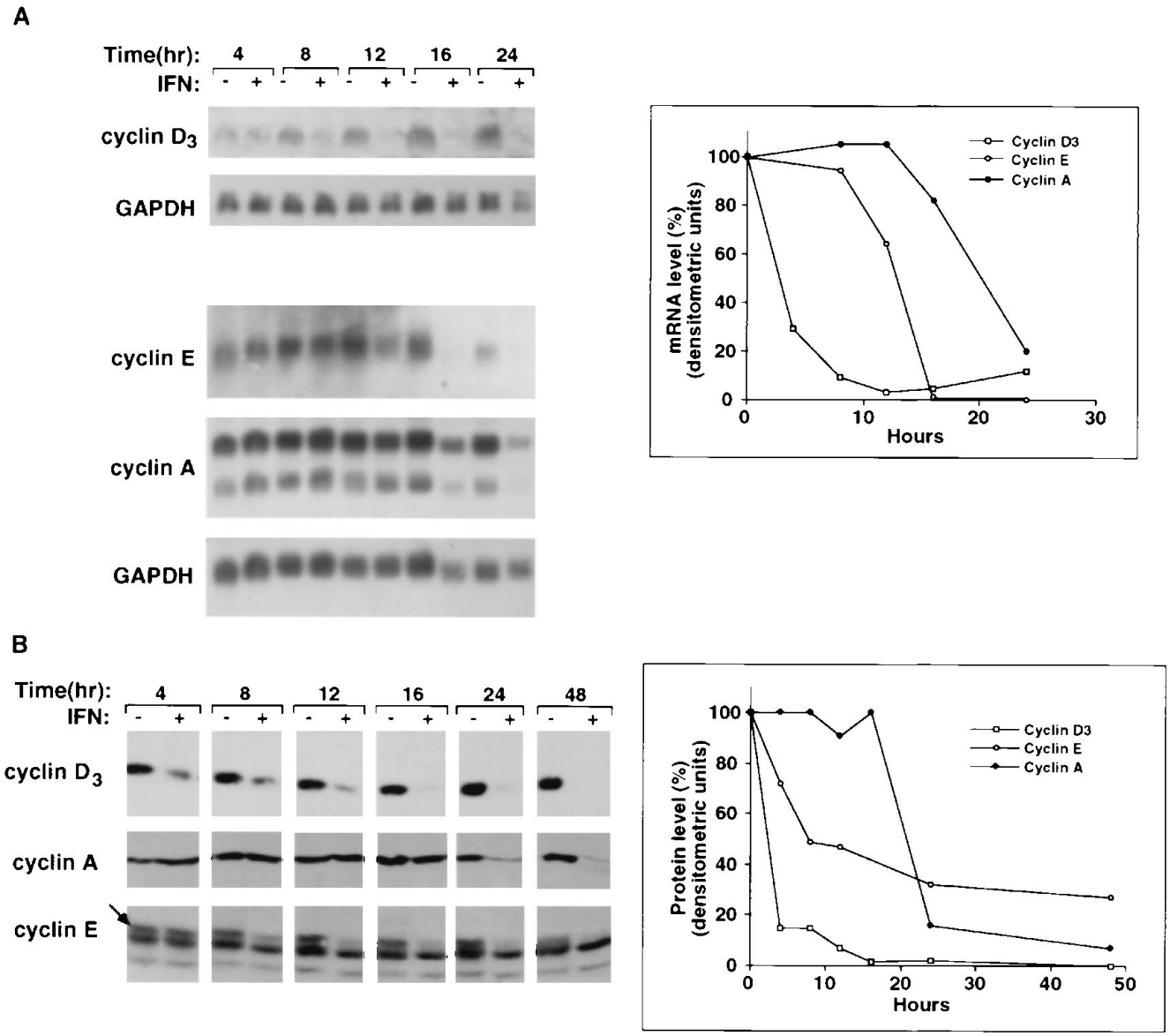

FIG. 2. Pattern of cyclin responses to IFN-α in Daudi cells. Exponentially growing cell cultures (1.5×10^5 cells per ml) were treated with IFN-α (+) or were left untreated (−) for different time intervals. (A) RNA expression as visualized on Northern blots. For cyclin D3 analysis, 20 μg of total RNA was hybridized to the murine *cyl 3* cDNA fragment; for cyclin E and cyclin A detections, poly(A)$^+$ RNA was purified from 150 μg of total cellular RNA and hybridized to a fragment of human cyclin E cDNA and subsequently to human cyclin A cDNA. The rat glyceraldehyde-3-phosphate dehydrogenase (GAPDH) cDNA was used as an internal control for the amount of RNA. Densitometric quantitation of the bands in the autoradiograms, after GAPDH corrections, is graphically presented. The zero time point is the average of all the corrected untreated-control points. (B) Immunoblot analysis of cyclin D3, cyclin E, and cyclin A proteins. The arrow in the cyclin E lane indicates the slowly migrating 55-kDa hyperphosphorylated form. Densitometric quantitation of the autoradiogram is graphically presented; the cyclin E curve corresponds to the slowly migrating band.

of cyclin A mRNA responses to the cytokine, i.e., maximal inhibition at 24 h (Fig. 2A and B).

Altogether, these results show that exposure of an asynchronous population of Daudi cells to IFN-α elicited a timely ordered response pattern in which cyclin D3 reduction was the first change to be detected. This was followed by the disappearance of the slowly migrating phosphorylated form of cyclin E and then by cyclin A protein reduction. The reduction of cyclin D3 and the loss of one of the cyclin E forms occurred before any changes in cell cycle distribution could be detected (Fig. 1B), suggesting that these responses are functional components of the cytokine-induced signaling events leading to cell cycle arrest.

IFN-α inhibits cyclin E- and cyclin A-associated kinase activities independently of its effect on cyclin expression. Histone H1 kinase assays were performed on immune complexes that were precipitated with anti-cyclin E or anti-cyclin A antibodies at various time intervals after IFN-α treatment. Both the cyclin E- and cyclin A-dependent kinases were rapidly suppressed by IFN-α (Fig. 3A and B). In the case of cyclin A, the reduction in kinase activity clearly preceded the slow decline in cyclin A protein levels (Fig. 3C), suggesting that IFN-α may induce a second rate-limiting event that restricts the kinase activity.

Examination of the cdk2 protein on immunoblots revealed that the expression levels of this catalytic subunit, which is common to both cyclin A- and E-associated kinases, remained

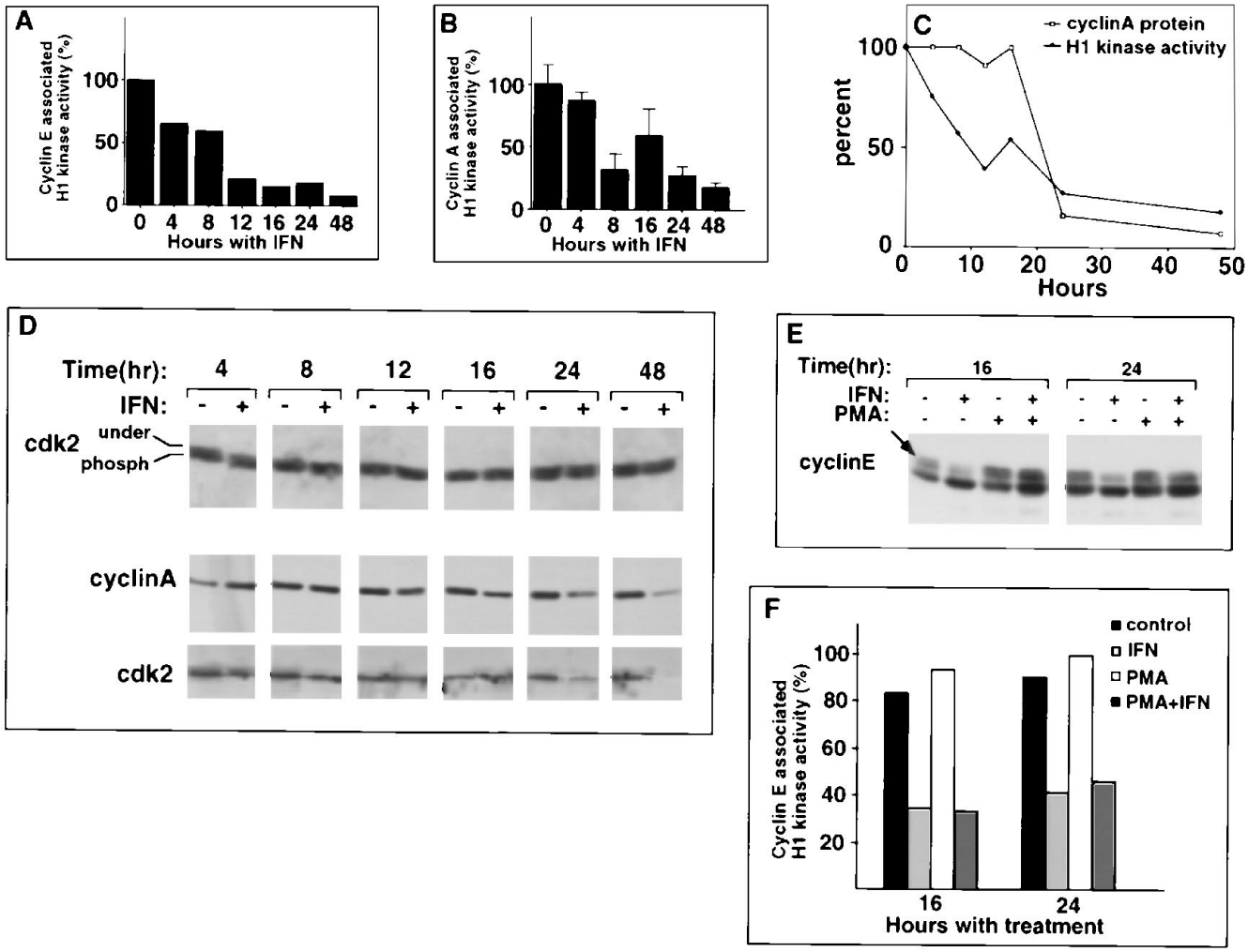

FIG. 3. IFN-α reduces the kinase activity of cyclin E- and cyclin A-containing complexes. Complexes immunoprecipitated with monoclonal antibodies directed against cyclin E (A) and polyclonal antibodies directed against cyclin A (B) were assayed for phosphorylation of histone H1 substrate. The quantitation of kinase activity was obtained by phosphorimager scanning of the histone H1 bands in gels; 100% activity corresponds to the activity of H1 kinase in untreated control cells. The histogram of the cyclin A-directed kinase activity represents the average of three independent experiments that were done on two sets of protein extracts. (C) Shown is a graphic representation of cyclin A protein levels and cyclin A-associated H1 kinase activity measured in the same cell lysate (the one depicted in Fig. 2B). (D) Protein extracts were prepared at different time intervals in the absence or the presence of IFN-α and tested for the formation of cyclin A-cdk2 complexes. To detect the two closely migrating forms of cdk2 (marked "under" and "phosph"), the fractionation of 100 μg of protein extract was performed on 26-cm slab gels (11% polyacrylamide) at a constant current of 60 mA and 4°C. The immunoblot was reacted with rabbit anti-human cdk2 antibodies; the result is shown in the top row of panel D. To detect cdk2 which is bound to cyclin A, immune complexes recovered from 400 μg of cell lysate after precipitation with anti-cyclin A antibodies were resolved by SDS-PAGE (11% gel) and immunoblotted. The gel shown in the middle row of panel D was probed with anti-cyclin A antibodies, and that shown in the bottom row was reacted with anti-cdk2 antibodies. (E) Daudi cells (2×10^5 per ml) were treated with IFN-α (300 U/ml) for 16 or 24 h or were left untreated; a portion of the cell culture was exposed for to PMA (5 ng/ml) 24 h before the start of the experiment, and the drug was retained during the subsequent period of IFN treatment. Protein analysis was performed as described in the legend to Fig. 2B. (F) The same cellular extracts that are described for panel E were analyzed for cyclin E-associated H1 kinase activity. Each histogram represents the average of three independent in vitro assays.

constitutive at the different time points following IFN-α treatment (Fig. 3D, top row). Also, cdk2 continued to migrate as a doublet on SDS-polyacrylamide gels, suggesting that the positive phosphorylation of this protein on threonine 160, which increases its mobility on gels (5, 20, 38), was not influenced by the cytokine treatment. To test for possible effects of IFN-α on cyclin A-cdk2 complex formation, immunoprecipitates were prepared with anti-cyclin A antibodies and, after gel fractionation and immunoblotting, were reacted with anti-cyclin A and anti-cdk2 antibodies. The levels of cdk2 that coimmunoprecipitated with the cyclin A protein remained unchanged at the early time points at which reduced kinase activity was displayed (Fig. 3D, middle and bottom rows, 4 to 16 h). Nor were the levels of cdc2 (cdk1) protein, which also forms complexes with cyclin A, reduced by IFN-α treatment at early time points (data not shown). At the 24- and 48-h time points, less cdk2 coimmunoprecipitated because of a reduction in cyclin A levels after long intervals of cytokine treatment. Altogether, these experiments suggested the existence of a second inhibitory effect of IFN-α that may either inactivate preexisting functional cyclin A-cdk complexes or interfere with the mechanisms that activate latent complexes after their formation.

In subsequent experiments we demonstrated that this second putative mechanism also operated at late time points of IFN-α treatment and that it affected both cyclin E- and cyclin A-associated kinase activities. In these experiments, we inter-

fered with the loss of the 55-kDa slowly migrating form of cyclin E and of cyclin A; nevertheless, significant reductions in the activities of both kinases by IFN-α were still observed. The uncoupling of these events was accomplished by depleting the cells of protein kinase C (PKC) activity by using a protocol involving the administration of phorbol myristate acetate (PMA) to cells, thus selectively abrogating the subset of IFN-α responses that depend on active PKC (36). We found here that depletion of PKC prevented the reduction by IFN-α of the slowly migrating form of the cyclin E protein at the 16- and 24-h time points (Fig. 3E). Yet, under these conditions, a marked reduction in the activity of the cyclin-E-directed kinase was still observed (Fig. 3F), indicating that the mechanism of inhibition was independent of cyclin E phosphorylation. Depletion of PKC from cells also interfered with the ability of IFN-α to reduce cyclin A protein expression (Fig. 4B, part a). As a consequence, the level of cyclin A-bound cdk2 in the depleted cells failed to decline at the 24-hour time point following cytokine treatment, in contrast to the reduction by IFN-α in cells that contain active PKC (Fig. 4B, part b). Nevertheless, the cyclin A-directed kinase activity in the depleted cells was lower at the 24-h time point IFN-α treatment because of this putative PKC-independent inhibitory mechanism (as detailed below and in Fig. 4C, part a).

Suppression of cdc25A expression mediates the effect of IFN-α on cyclin E- and cyclin A-associated kinase activities. We next tested whether the inhibitory effects of IFN-α on the activities of preexisting cyclin E- and cyclin A-cdk2 complexes could be mediated by regulating the negative phosphorylation of cdk2 on tyrosine 15. Examination of cdc25A, the tyrosine phosphatase that removes the phosphate residue from this site, revealed that this activating enzyme is tightly regulated by IFN-α in Daudi cells. The cdc25A mRNA and protein levels were sharply reduced a few hours after treatment with IFN-α (Fig. 4A), suggesting that latent cdk2 complexes may not be activated after IFN-α treatment. Interestingly, the depletion of PKC did not abrogate the cdc25A responses to IFN-α (Fig. 4B, part a), a finding that was consistent with the sustained inhibition of the kinase activity under these conditions.

The strong and rapid inhibitory effect of IFN-α on the expression of cdc25A protein and the resistance of this inhibition to PKC depletion suggested that this event may be the primary mechanism accounting for the rapid reduction in the activities of cyclin E- and cyclin A-cdk2 kinase complexes. In order to test this possibility directly, in vitro phosphatase assays were performed on inhibited cyclin-cdk immune complexes in an attempt to restore their kinase activities after IFN-α treatment. A protein consisting of GST fused to the catalytic domain of yeast $p80^{cdc25}$ was used in these assays. This domain is highly conserved among the different cdc25 homologs and was reported to possess tyrosine phosphatase activity when expressed in bacterial systems (27). The phosphatase activity of the recombinant protein was calibrated by using *p*-nitrophenyl-phosphate as a substrate and measuring the release of *p*-nitrophenolate ions at 410 nm (37). Extracts prepared from IFN-α-treated cells under conditions in which the cyclins themselves were not affected (because of PKC depletion) were immunoprecipitated with anti-cyclin A (at 24 h), anti-cdk2 (at 16 h), or anti-cyclin E (at 16 h) antibodies and assayed for kinase activity (Fig. 4C, parts a, b, and c, respectively). The untreated cells were similarly depleted of PKC activity. Prior to the kinase assay, the immune complexes were incubated with the GST-cdc25 fusion protein. The mock incubation of the immunoprecipitates (with GST alone) revealed the expected reduction of histone H1 phosphorylation by IFN-α. However, the reduction of histone H1 phosphorylation by IFN-α was completely abolished after incubation of these different complexes with the catalytic domain of cdc25 (Fig. 4C, parts a, b, and c). In fact, the kinase activity of the phosphatase-treated complexes that were immunoprecipitated with anti-cyclin E antibodies was even higher in the IFN-α-treated cells than in the control cells (Fig. 4C, part c), which is consistent with the increase in total cyclin E protein that is seen in IFN-α-treated PKC-depleted cells at 16 h (Fig. 3E). The same analysis was done on cdk2 immune complexes which were prepared 9 h after addition of IFN-α without a prior PKC depletion step (cyclin A levels are not rate limiting at this early time point, and therefore PMA pretreatment was not required). Here again, the phosphatase treatment completely abolished the IFN-α-mediated inhibition of cdk2 activity, and the kinase levels were indistinguishable from those measured in untreated control cells (Fig. 4D). It should be noted that some latent cdk2 complexes also exist in exponentially growing cells because of the late activation of cdc25A during the G_1 phase (15, 17). As a consequence, incubation with the phosphatase augmented the kinase activity in the nontreated samples to some extent. Yet, the extent of stimulation by cdc25 was always much higher in the IFN-α-treated cells, resulting in the complete abrogation of the IFN-α-mediated reductions and in the restoration of cyclin-cdk2 activity to control levels (Fig. 4D). It was therefore concluded from these experiments that the cdc25A gene is a crucial target for IFN-α signaling and that its rapid suppression prevents the activation of preexisting latent cyclin-cdk2 complexes.

A prolonged delay precedes recovery of cyclin and cdc25A expression and reentry into S phase following release from IFN-α arrest. We found that the antiproliferative effects of IFN-α in this system were reversible and that Daudi cells reentered the cell cycle upon removal of the cytokine after a lag period of approximately 48 h. The first cell doubling was asynchronous and occurred between 48 and 96 h after IFN-α release; it was followed by a second, accelerated round of replication, corresponding to about 60% of the normal doubling time of Daudi cells (Fig. 5A). A control culture that was subjected to similar washes displayed the normal doubling time of 24 h with no detectable lag periods (data not shown). In several experiments, cell death was apparent to varying extents during the lag period after withdrawal of the cytokine (e.g., the drop in cell number during the lag period in Fig. 5A), yet the timing of cell cycle reentry and of restoration of cyclin expression was not influenced by the extent of cell death.

Reentry into S phase following the release from IFN-α arrest was measured by double staining with BrdU and PI (Fig. 5A). Consistent with the cell proliferation kinetics, a prolonged lag preceded a rather asynchronous entry into S phase after the removal of IFN-α. It is noteworthy that a detailed examination of the first few hours after release from the cytokine arrest failed to reveal a detectable escape into S phase, indicating that not even a small fraction of cells were retained by IFN-α at a late-G_1 checkpoint (Fig. 5A). Instead, during the first 24 h after withdrawal of the cytokine, the percentage of cells found in S phase continued to decline, from 10 to 20% at the time of cytokine withdrawal (time zero in Fig. 5A) to minimum values of approximately 5%. Performance of BrdU pulse-labeling of cells immediately after withdrawal of the cytokine, followed by 24- and 48-h chase periods, indicated that the label reappeared in the 2*n*-DNA-containing arrested population (data not shown). This suggests that the fraction of cells that still incorporated BrdU after 48 h of treatment (time zero in Fig. 5A) were already committed to arrest and eventually joined the

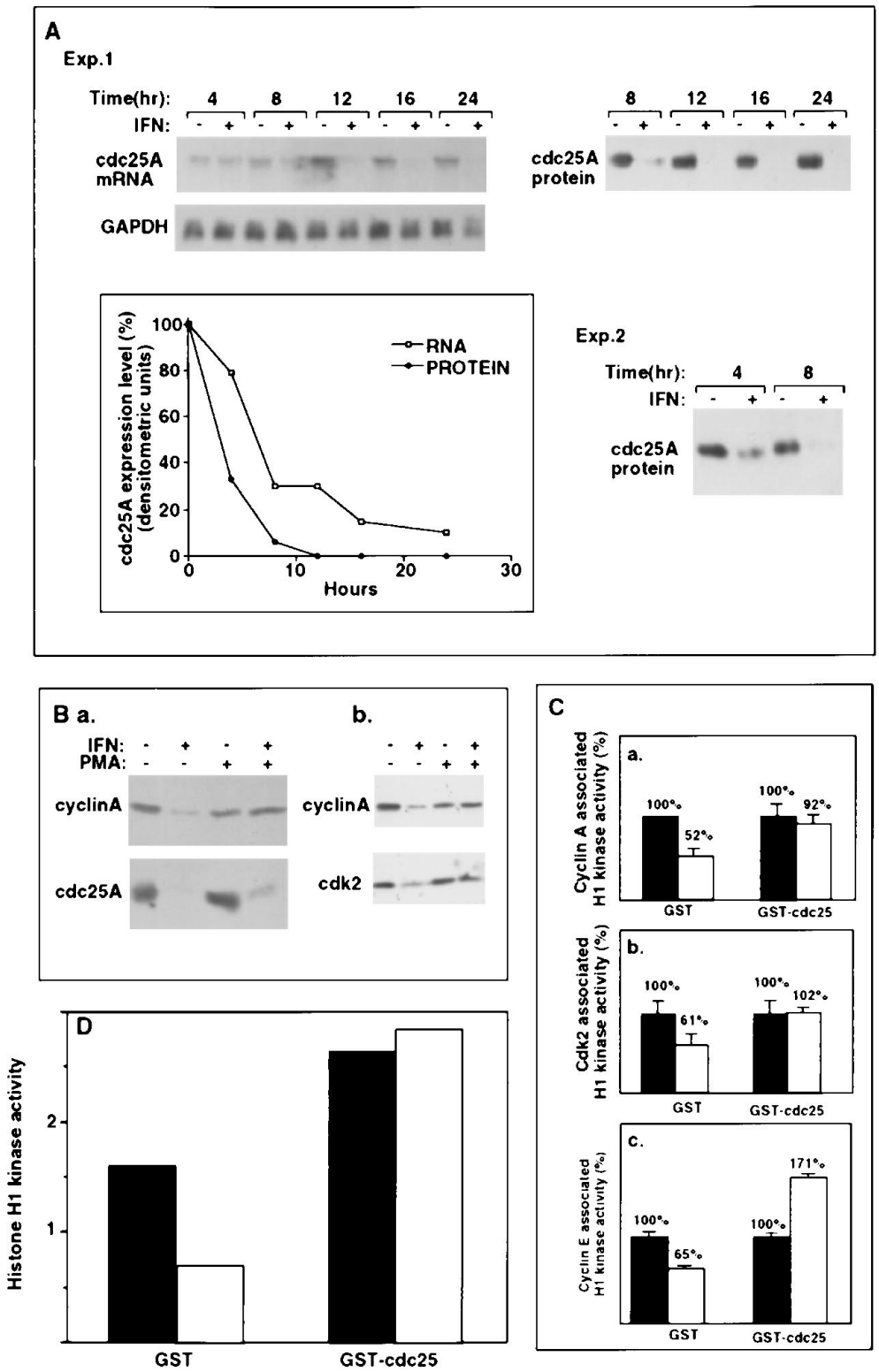

FIG. 4. IFN-α prevents cdk2 activation by suppressing cdc25A phosphatase expression. (A) Northern and Western blot analyses of cdc25A RNA and protein. Daudi cells were treated with human IFN-α (300 U/ml) for different time intervals or were left untreated. Total RNA and cellular proteins were analyzed. For detection of cdc25A mRNA, 20 μg of total RNA was electrophoresed on a gel, blotted, and hybridized to the 2.5-kb *Eco*RI fragment containing the coding sequence of the cdc25A gene. The immunoblot analysis of the cdc25A protein was done with affinity-purified polyclonal antibodies against cdc25A. The results of two independent experiments (Exp. 1 and 2) are presented. Densitometric quantitations of both RNA and protein are graphically presented. The zero time point (100%) corresponds to an average value of the different untreated control extracts that are presented in the autoradiograms. See the legend to Fig. 2A for an explanation of the GAPDH data. (B) cdc25A reduction by IFN-α is resistant to PKC depletion. Daudi cells (3×10^5 per ml) were treated with IFN-α (300 U/ml) for 24 h. A portion of the cell culture was pretreated for 24 h with PMA (5 ng/ml), and the drug was retained during the subsequent period of IFN treatment. (Part a) A sample containing 100 μg of protein was analyzed in each lane; immunoblots were reacted with anti-cyclin A antibodies and with anti-cdc25A antibodies. (Part b) To detect cdk2 which was bound to cyclin A, anti-cyclin

pool of resting cells even though IFN-α was withdrawn. Together, these data indicate that as a result of the effects of IFN-α, cells are maintained in a nonproliferative state from which the return to the cell cycle is a long-term process.

The pattern of restoration of cyclin expression during the return to the cell cycle was determined by immunoblot analysis and compared with the kinetics of resumption of c-*myc* expression. Cell lysates were prepared from logarithmic-phase cultures, from cells treated with IFN-α for 48 h, and at different time points after cytokine withdrawal (C, 0, and 12 to 96 h, respectively, in Fig. 5B and C). An IFN-responsive immediate-early gene that codes for a short-half-life protein, IRF-1 (13), was used as a marker to confirm that cell surface signaling was terminated efficiently after ligand removal at time zero (note that the IRF-1 protein that was induced by IFN-α disappeared at the earliest time point after cytokine removal [Fig. 5B, 12-h point]).

One striking finding was a marked difference in the behavior of the c-*myc* and cyclin genes following release from IFN-α arrest. The c-myc protein levels, which were reduced to below detection limits by IFN-α, returned to control levels as early as 12 h after withdrawal of the cytokine, which is consistent with the decay in IFN-α signaling (Fig. 5B). In contrast, the restoration of cyclin expression (i.e., cyclins D3 and A) in these same extracts occurred much later and was rather asynchronous. The levels of cyclin D3 protein first reappeared 36 h after cytokine withdrawal and gradually increased thereafter, reaching control levels by 60 h. The cyclin A protein started to reappear later, at 60 h after cytokine withdrawal, and reached control levels at 72 to 96 h (Fig. 5B and C). The resumption of cdc25A protein expression was also very slow and asynchronous, and the appearance of the 55-kDa phosphorylated form of cyclin E followed similar kinetics (Fig. 5C). The cdk2 protein was constitutively expressed in the IFN-α-treated cells, and its levels were invariant after cytokine withdrawal.

DISCUSSION

The capability of growth-inhibitory cytokines to cause the arrest of proliferation of certain cultured cells provides a powerful tool for studying the negative control of the cell cycle. In most cases studied so far, treatment with the cytokine culminated in the accumulation of nondividing cells with 2*n* DNA content. This characterizes the response of lung epithelial cells, keratinocytes, and myeloid cell lines to TGF-β1 and the response of several hematopoietic cell lines to IFNs and interleukin-6 (1, 6, 16, 19, 23, 34, 35). Yet, more detailed analyses of these systems, including the present study, show diversity in terms of the type of cell cycle arrest and the mechanisms by which cytokine signaling is integrated into the basic machinery of the cell cycle. For instance, in systems in which TGF-β1 was added to synchronized epithelial cells after their release from serum deprivation, a late-G_1 arrest was documented (10, 16, 21, 29). Mechanistically, in these systems, the effects of TGF-β1 were attributed to a few events that operate in a colinear pathway, such as suppression of cdk4 synthesis and induction of $p15^{ink4B}$, and that each led to the displacement of $p27^{kip-1}$ and its binding to cdk2 complexes (9, 12, 30, 35). In contrast, it is shown here that the nature of the cell cycle arrest that develops when asynchronous Daudi cell cultures are exposed to IFN-α is quite different, as are the components of the basic cell cycle machinery that are being targeted.

Two major downstream targets of IFN-α were identified in this work: the cyclin D3 and *cdc25A* genes, which were both suppressed at the mRNA and protein levels before any change in cell cycle distribution could be detected. The suppression of cdc25A by IFN-α provides the first documented example of this phosphatase being tightly regulated by an external growth-inhibitory signal. It was previously shown that removal of the phosphate from tyrosine 15, which is located next to the ATP binding site, is critical for activation of the cdk2 catalytic subunit of cyclin-cdk2 complexes (11, 15). Thus, while the obvious outcome of cyclin D3 suppression would be the shutting off of cyclin D-associated cdk4 and cdk6 kinase activities, the suppression of cdc25A prevented the activation of cdk2-cyclin E and cdk2-cyclin A complexes, which both continued to accumulate during the first few hours of IFN-α treatment. Later, cyclin A itself became rate limiting in the system, thus introducing a level of redundancy to the regulation of cyclin A-associated kinase activity by IFN-α. The depletion of PKC from cells was a powerful tool with which to confront the redundancy issue, since this kinase interfered with cyclin A suppression without preventing the cdc25A responses to IFN-α and also prevented the loss of the 55-kDa hyperphosphorylated cyclin E species. This provided an appropriate context in which to test directly the functional importance of cdc25A in negative growth signaling by IFN-α. Under these specific conditions, we abrogated the reduction by IFN-α of cdk2-cyclin E and cdk2-cyclin A activities through in vitro phosphatase treatment. Thus, cdc25A regulation is the critical early step through which IFN-α signaling reduces the activity of cdk2-cyclin kinases. It should be noted that kinase inhibition assays, which screen for cdk inhibitors that operate in *trans*, were also performed in the Daudi–IFN-α system. In these experiments, extracts prepared from untreated control cells were mixed with boiled extracts derived from IFN-α-treated Daudi cells, since all the cdk inhibitors that have been identified so far were reported to be heat stable (7). Incubation was followed by immunoprecipitation of cdk2 complexes and analysis of their associated kinase activity, as detailed in a previous work (4). Boiled extracts from M1 cells that had been transfected with the temperature-sensitive p53 gene (41) and shifted to the permissive temperature (to induce the $p21^{waf-1}$ cdk inhibitor) were used as positive controls in these mixing experiments. The results indicated that IFN-α did not activate the putative heat-stable cdk inhibitors capable of suppressing in *trans* the cdk-cyclin complexes

A immunoprecipitates were recovered from 400 μg of the same protein lysate as described for part a, resolved by SDS-PAGE (11% gel), and immunoblotted. The upper part of the gel was probed with anti-cyclin A antibodies, and the lower part was reacted with anti-cdk2 antibodies. (C) In vitro phosphatase treatment abolishes the IFN-α-induced reduction of cyclin-cdk2 kinase activity in PKC-depleted cells. Cell extracts were immunoprecipitated with the various antibodies, and the washed immune complexes were divided into two portions and incubated for 30 min at 30°C with GST alone or GST-cdc25 before the assay of histone H1 phosphorylation was performed. (Part a) PMA-pretreated cells were either treated with IFN-α for 24 h (empty bars) or not treated with IFN-α (black bars) and immunoprecipitated with anti-cyclin A antibodies. (Parts b and c) PMA-pretreated cells were either treated with IFN-α for 16 h (empty bars) or not treated with IFN-α (black bars) and immunoprecipitated with anti-cdk2 or anti-cyclin E antibodies, respectively. The data for parts a, b, and c represent the averages of three different experiments. The values are presented as the percentage of H1 histone kinase activity in the treated sample relative to that in the control (no IFN-α) sample of each pair. (D) In vitro phosphatase treatment abolishes the early reduction by IFN-α of cdk2-associated kinase activity. Extracts were prepared from cells which had either been treated for 9 h with IFN-α (empty bars) or had not undergone IFN-α treatment (black bars). The extracts were then immunoprecipitated with anti-cdk2 antibodies. The washed immune complexes were incubated with recombinant GST or GST-cdc25 proteins as described for panel C. Histone H1 kinase activity was quantitated with a phosphorimager and is expressed in arbitrary units.

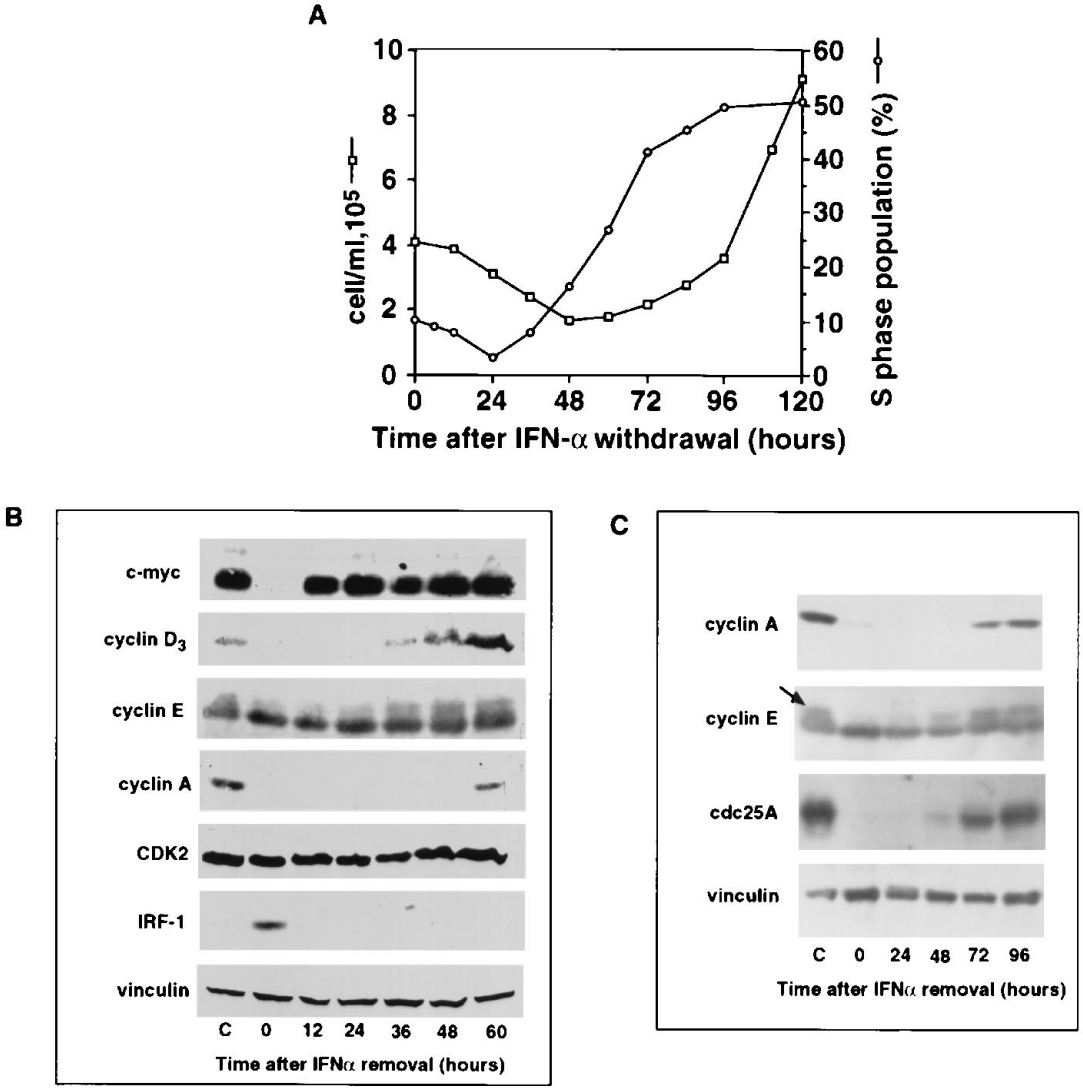

FIG. 5. Kinetics and recovery of molecular events upon release from IFN arrest. (A) Exponentially growing cells were treated with IFN-α for 48 h, washed, and recultured in fresh medium (time 0). Cell samples from the indicated time points were counted and subjected to FACS analysis as described in the legend to Fig. 1A. □, proliferation curve as determined by viable cell counts; ○, percentage of cells engaged in active DNA replication as determined by BrdU-PI double staining. (B and C) Immunoblot analysis of cell extracts prepared in two different experiments at the indicated time points (0, time of release from IFN-α; C, exponentially growing control cells). The immunoblots were reacted with antibodies prepared against the indicated proteins.

(data not shown). The inhibitory effects of IFN-α on cdk2 activity are therefore restricted to the aforementioned mechanism that retains the negative phosphorylation.

A number of criteria suggest that IFN-α induces in this system a transition to a G_0-like state rather than imposing a late-G_1 block. First, cytokine-arrested cells displayed on average a reduced protein content and cell size compared with G_1 cells in cycling populations. Second, it appears that IFN-α induces in Daudi cells a wide array of molecular changes that function in parallel, rather than inducing a single linear pathway, which may be sufficient for a block in G_1 transit. In addition to the simultaneous inhibition of cyclin-dependent kinases shown here, which may be responsible for the previously reported suppression of pRB phosphorylation (34), IFN-α downregulates the c-*myc* gene with similar temporal kinetics and reduces the DNA-binding activity of E2F by mechanisms that are independent of the cyclin-pRB responses (25). Interestingly, while the suppression of the cyclin A protein was PKC dependent, the cyclin D3 protein continued to be inhibited by IFN-α in PKC-depleted cells (data not shown), a finding which further stresses the existence of multiple arms in the signaling pathways, among which only a few depend on active PKC. A number of proliferative restrictions are therefore independently imposed by the cytokine. The third property that supports the cell cycle exit concept is the length of time required to emerge from the resting state and to reenter the replicative cycle. A prolonged delay, equivalent to the duration of almost two cell cycles, preceded entry into S phase upon release from IFN-α arrest. During this lag period, the expression of cyclin D3, cyclin A, and cdc25A remained silent, in spite of the fact that the negative external constraint that initially suppressed their expression had been removed. The last supporting feature relates to the finding that the IFN-α-arrested cells did not accumulate as homogeneous cell populations. Individual IFN-α-treated 2*n*-DNA-containing cells differed in their protein content and in the timing of resumption

of cyclin expression, resulting in a rather asynchronous pattern of entry into S phase after cytokine withdrawal.

The heterogeneity in protein content and the slow and asynchronous profile of resumption of cell proliferation both argue against the concept of accumulation at a common restriction point in the G_1 phase of the cell cycle. For example, in TGF-β-1-treated cells that were arrested in late G_1, the reentry into S phase was rapid and synchronous (about 2 h from release [16]). Also, the recovery of epithelial and myeloid cells from proliferation arrest imposed by serum or growth factor deprivation was more synchronous and significantly shorter (i.e., 10 to 15 h) (10, 21, 24, 29) than that described in this work. Interestingly, the recovery of proliferation in normal quiescent primary lymphocytes is of the prolonged and asynchronous type, similar to the pattern of release from IFN-α arrest. For instance, DNA replication was first detected in phytohemagglutinin- or anti-CD2-activated human T lymphocytes as late as 30 to 36 h after stimulation, and the fraction of S-phase cells then increased gradually during the next 2 to 4 days (2, 3, 26). This delayed pattern may be, therefore, indicative of normal quiescent lymphocytes, thus suggesting that the Daudi cells, in spite of their tumorigenic origin, still carry the intact mechanisms required for cell cycle exit upon exposure to the appropriate antimitogenic signals.

One of the key findings concerning the reentry into S phase after release from the IFN-α-induced cell cycle arrest relates to the uncoupling between cyclins and c-*myc*. While protein and mRNA levels of cyclin D3 and c-*myc* rapidly declined with almost identical kinetics after the exposure of Daudi cells to IFN-α (for details on the kinetics of c-*myc* responses, see reference 34), the resumption of cyclin D3 gene expression after release from arrest was strikingly delayed compared with that of c-*myc*. The c-myc protein returned to normal levels characteristic of proliferating cells within 12 h, i.e., concomitant with the decay in IFN-α signaling. In contrast, cyclin D3 protein remained suppressed for almost 36 h after IFN-α had been removed from the cell surface. In addition, unlike that of c-myc, cyclin D3 restoration was rather asynchronous, gradually increasing between 36 and 60 h after removal of IFN-α. The restoration of cyclin A and cdc25A expression also displayed this slow and asynchronous pattern. It is possible that cyclin genes, unlike c-*myc*, remain under the negative control of IFN-α long after its removal and that this control is mediated by some of the IFN-α-responsive immediate-early genes that may persist for extended periods of time. Yet, this simple possibility is not compatible with the asynchronous pattern of reexpression of cyclins. Alternatively, the suppression of G_1 cyclin genes (but not of c-*myc*) during the recovery period may depend not on IFN signaling but rather on novel intrinsic restriction(s) imposed, for example, by the reduced cell size or protein content of the arrested cells.

In conclusion, this work provides the first example of a bidirectional transition between cycling cells and a G_0-like arrest being imposed by the administration and removal of a single growth-inhibitory cytokine.

ACKNOWLEDGMENTS

We thank G. Draetta for the anti-cyclin A polyclonal antibodies and J. Chebath for the anti-IRF-1 polyclonal antibodies. Special thanks to A. Sharp and E. Ariel for their assistance in the FACS analyses.

This work was supported by the Israel Science Foundation, administered by the Israel Academy of Sciences and Humanities; the DKFZ-Weizmann joint research program; NIH grant GM46006; and the Council on Tobacco Research grant 3165. A.K. is an Incumbent of the Helena Rubinstein Chair of Cancer Research. D.R. was supported by a Senior Postdoctoral Fellowship from the American Cancer Society, California Division.

REFERENCES

1. **Burke, L. B., A. Bybee, and N. S. B. Thomas.** 1992. The retinoblastoma protein is partially phosphorylated during early G1 in cycling cells but not in G1 cells arrested with α-interferon. Oncogene **7:**783–788.
2. **DeCaprio, J. A., Y. Furukawa, F. Ajchenbaum, J. D. Griffin, and D. M. Livingston.** 1992. The retinoblastoma-susceptibility gene product becomes phosphorylated in multiple stages during cell cycle entry and progression. Proc. Natl. Acad. Sci. USA **89:**1795–1798.
3. **DeCaprio, J. A., J. W. Ludlow, D. Lynch, Y. Furukawa, J. Griffin, H. Piwnica-Worms, C. M. Huang, and D. M. Livingston.** 1989. The product of the retinoblastoma susceptibility gene has properties of a cell cycle regulatory element. Cell **58:**1085–1095.
4. **Dulic, V., W. K. Kaufmann, S. J. Wilson, T. D. Tlsty, E. Lees, J. W. Harper, S. J. Elledge, and S. I. Reed.** 1994. p53-dependent inhibition of cyclin-dependent kinase activities in human fibroblasts during radiation-induced G1 arrest. Cell **76:**1013–1023.
5. **Dulic, V., E. Lees, and S. I. Reed.** 1992. Association of human cyclin E with a periodic G1-S phase protein kinase. Science **257:**1958–1961.
6. **Einat, M., D. Resnitzky, and A. Kimchi.** 1985. Close link between reduction of c-*myc* expression by interferon and G0/G1 arrest. Nature (London) **313:** 597–600.
7. **Elledge, S. J., and J. W. Harper.** 1994. Cdk inhibitors: on the threshold of checkpoints and development. Curr. Opin. Cell Biol. **6:**847–852.
8. **Evan, G. I., G. K. Lewis, G. Ramsay, and J. M. Bishop.** 1985. Isolation of monoclonal antibodies specific for human c-*myc* proto-oncogene product. Mol. Cell. Biol. **5:**3610–3616.
9. **Ewen, M. E., H. K. Sluss, L. L. Whitehouse, and D. M. Livingston.** 1993. TGF-β inhibition of Cdk4 synthesis is linked to cell cycle arrest. Cell **74:** 1009–1020.
10. **Geng, Y., and R. A. Weinberg.** 1993. Transforming growth factor beta effects on expression of G1 cyclins and cyclin-dependent protein kinases. Proc. Natl. Acad. Sci. USA **90:**10315–10319.
11. **Gu, Y., J. Rosenblatt, and D. O. Morgan.** 1992. Cell cycle regulation of CDK2 activity by phosphorylation of Thr160 and Tyr15. EMBO J. **11:**3995–4005.
12. **Hannon, G. J., and D. Beach.** 1994. $p15^{ink4B}$ is a potential effector of TGF-β-induced cell cycle arrest. Nature (London) **371:**257–260.
13. **Harada, H., T. Fujita, M. Miyamoto, Y. Kimura, M. Maruyama, A. Furia, T. Miyata, and T. Taniguchi.** 1989. Structurally similar but functionally distinct factors bind to the same regulatory elements of IFN and IFN-inducible genes. Cell **58:**729–739.
14. **Hinds, P. W.** 1995. The retinoblastoma tumor suppressor protein. Curr. Opin. Genet. Dev. **5:**79–83.
15. **Hoffmann, I., G. Draetta, and E. Karsenti.** 1994. Activation of the phosphatase activity of human cdc25A by a cdk2-cyclin E dependent phosphorylation at the G1/S transition. EMBO J. **13:**4302–4310.
16. **Howe, P. H., G. Draetta, and E. B. Leof.** 1991. Transforming growth factor β1 inhibition of $p34^{cdc2}$ phosphorylation and histone H1 kinase activity is associated with G1/S-phase growth arrest. Mol. Cell. Biol. **11:**1185–1194.
17. **Jinno, S., K. Suto, A. Nagata, M. Igarashi, Y. Kanaoka, H. Nojima, and H. Okayama.** 1994. Cdc25A is a novel phosphatase functioning early in the cell cycle. EMBO J. **13:**1549–1556.
18. **Kimchi, A.** 1992. Cytokine triggered molecular pathways that control cell cycle arrest. J. Cell. Biochem. **50:**1–9.
19. **Kimchi, A., D. Resnitzky, R. Ber, and G. Gat.** 1988. Recessive genetic deregulation abrogates c-*myc* suppression by interferon and is implicated in oncogenesis. Mol. Cell. Biol. **8:**2828–2836.
20. **Koff, A., M. Ohtsuki, K. Polyak, J. M. Roberts, and J. Massague.** 1993. Negative regulation of G1 in mammalian cells: inhibition of cyclin E-dependent kinase by TGF-beta. Science **260:**536–539.
21. **Laiho, M., J. A. DeCaprio, J. W. Ludlow, D. M. Livingston, and J. Massague.** 1990. Growth inhibition by TGF-β is linked to suppression of retinoblastoma protein phosphorylation. Cell **62:**175–185.
22. **Lees, E., B. Faha, V. Dulic, S. I. Reed, and E. Harlow.** 1992. Cyclin/cdk2 and cyclin A/cdk2 kinases associate with p107 and E2F in a temporally distinct manner. Genes Dev. **6:**1874–1885.
23. **Levy, N., E. Yonish-Rouach, M. Oren, and A. Kimchi.** 1993. Complementation by wild-type p53 of interleukin-6 effects on M1 cells: induction of cell cycle exit and cooperativity with c-*myc* suppression. Mol. Cell. Biol. **13:**7942–7952.
24. **Matsushime, H., M. F. Roussel, R. A. Ashmun, and C. J. Sherr.** 1991. Colony-stimulating factor 1 regulates novel cyclins during the G1 phase of the cell cycle. Cell **65:**701–713.
25. **Melamed, D., N. Tiefenbrun, A. Yarden, and A. Kimchi.** 1993. Interferons and interleukin-6 suppress the DNA-binding activity of E2F in growth-sensitive hematopoietic cells. Mol. Cell. Biol. **13:**5255–5265.
26. **Meuer, S. C., R. E. Hussey, M. Fabbi, D. Fox, O. Acuto, K. A. Fitzgerald, J. C. Hodgdon, J. P. Protentis, S. F. Schlossman, and E. L. Reinherz.** 1984. An alternative pathway of T-cell activation: a functional role for the 50 kd T11 sheep erythrocyte receptor protein. Cell **36:**897–906.
27. **Millar, J. B., C. H. McGowan, G. Lenaers, R. Jones, and P. Russell.** 1991. p80cdc25 mitotic inducer is the tyrosine phosphatase that activates p34cdc2

kinase in fission yeast. EMBO J. **10:**4301–4309.
28. **Pagano, M., R. Pepperkok, F. Verde, W. Ansorge, and G. Draetta.** 1992. Cyclin A is required at two points in the human cell cycle. EMBO J. **11:**961–971.
29. **Pietenpol, J. A., R. W. Stein, E. Moram, P. Yaluk, R. Schlegel, R. M. Lyons, M. R. Pittelkow, K. Munger, P. M. Howley, and H. L. Moses.** 1990. TGF-β inhibition of c-myc transcription and growth in keratinocytes is abrogated by viral transforming proteins with pRB binding domains. Cell **61:**777–785.
30. **Polyak, K., M. H. Lee, B. H. Erdjument, A. Koff, J. M. Roberts, P. Tempst, and J. Massague.** 1994. Cloning of p27Kip1, a cyclin-dependent kinase inhibitor and a potential mediator of extracellular antimitogenic signals. Cell **78:**59–66.
31. **Reed, S. I.** 1992. The role of p34 kinases in the G1 to S-phase transition. Annu. Rev. Cell Biol. **8:**529–561.
32. **Resnitzky, D., M. Gossen, H. Bujard, and S. I. Reed.** 1994. Acceleration of the G_1/S phase transition by expression of cyclins D1 and E with an inducible system. Mol. Cell. Biol. **14:**1669–1679.
33. **Resnitzky, D., and A. Kimchi.** 1991. Deregulated c-*myc* expression abrogates the interferon- and interleukin 6-mediated G0/G1 cell cycle arrest but not other inhibitory responses in M1 myeloblastic cells. Cell Growth Differ. **2:**33–41.
34. **Resnitzky, D., N. Tiefenbrun, H. Berissi, and A. Kimchi.** 1992. Interferons and interleukin 6 suppress phosphorylation of the retinoblastoma protein in growth-sensitive hematopoietic cells. Proc. Natl. Acad. Sci. USA **89:**402–406.
35. **Reynisdottir, I., K. Polyak, A. Iavarone, and J. Massague.** 1995. Kip/Cip and Ink4 Cdk inhibitors cooperate to induce cell cycle arrest in response to TGF-beta. Genes Dev. **9:**1831–1845.
36. **Tiefenbrun, N., and A. Kimchi.** 1991. The involvement of protein kinase C in mediating growth suppressive signals of interferons in hematopoietic cells. Oncogene **6:**1001–1007.
37. **Tonks, N. K., C. D. Diltz, and E. H. Fischer.** 1988. Purification of the major protein-tyrosine phosphatase of human placenta. J. Biol. Chem. **263:**6722–6730.
38. **Tsai, L. H., E. Lees, B. Faha, E. Harlow, and K. Riabowol.** 1993. The cdk2 kinase is required for the G1-to-S transition in mammalian cells. Oncogene **8:**1593–1602.
39. **Won, K.-A., and S. I. Reed.** EMBO J., in press.
40. **Yarden, A., and A. Kimchi.** 1986. Tumor necrosis factor reduces c-myc expression and cooperates with IFN-γ in HeLa cells. Science **243:**1419–1421.
41. **Yonish-Rouach, E., D. Resnitzky, Y. Lotem, L. Sachs, A. Kimchi, and M. Oren.** 1991. Wild type p53 induces apoptosis of myeloid leukaemic cells that is inhibited by interleukin-6. Nature (London) **352:**345–347.